Volume 18, No 4 | International Journal of Radiation Research, October 2020

Biokinetic modelling of ^{89}Zr-labelled monoclonal antibodies for dosimetry assessment in humans

H.M.H. Zakaly[1,2*], M.Y.A. Mostafa[1,3], M. Zhukovsky[4]

[1]*Department of Experimental Physics, Institute of Physics and Technology, Ural Federal University, Yekaterinburg, Russia*
[2]*Physics Department, Faculty of Science, Al-Azhar University, Assuit Branch, Assuit, Egypt*
[3]*Minia University, Faculty of Science, Department of Physics, El-Minia, Egypt*
[4]*Institute of Industrial Ecology UB RAS, Ekaterinburg, Russia*

► ***Original article***

Corresponding authors:
Hesham Zakaly, M.H., Ph.D.,
E-mail:
h.m.zakaly@azhar.edu.eg

Revised: November 2019
Accepted: January 2020

Int. J. Radiat. Res., October 2020; 18(4): 825-833

DOI: 10.18869/acadpub.ijrr.18.4.825

ABSTRACT

Background: Monoclonal antibodies have confirmed their merit as biotherapeutics across a wide spectrum of diseases, including cancer, heart disease, infection, and immune disorders. **Materials and Methods:** The dynamics of ^{89}Zr-labelled monoclonal antibodies (MAb) after injection into the human body are modelled. This modified biokinetic model can be used for dose assessment not only for ^{89}Zr-labelled MAb tumour visualization but also for diagnostic and radiation therapy with other MAb-labelled radionuclides. The created modified biokinetic model is based on experimental data from the literature. The cumulative ^{89}Zr activity in organs and tissues per Bq of administered activity is calculated with the WinAct program. **Results:** For the organs receiving the highest radiation exposure, the average absorbed doses were estimated with IDAC 2.1 software. The results from the modelled calculations are compared with new published experimental diagnostic results from real patients. The calculations reveal that the organs which received the highest dose were the spleen, liver, kidneys, and red bone marrow (doses of 1.54, 1.33, 0.81 and 0.82 mGy/MBq, respectively). In the modified biokinetic model, the organs exhibiting the highest dose were the liver, gallbladder wall, spleen, pancreas, and kidneys (at 1.07, 0.77, 0.70, 54 and 0.44 mGy/MBq, respectively), when the injection was associated with monoclonal antibodies. **Conclusion:** The developed biokinetic model is in good agreement with direct measurements and can be considered a first step for simulating the radiopharmaceutical dosimetry of the ^{89}Zr isotope.

Keywords: *PET visualization, internal exposure, zirconium-89, monoclonal antibodies, absorbed dose.*

INTRODUCTION

Monoclonal antibodies have proven their worth as biotherapeutics across a wide spectrum of diseases, including cancer, heart disease, infection, and immune disorders [1–4], as is evidenced by the growing list of MAbs that have been approved by the US Food and Drug Administration (FDA) and the European Medicines Agency (EMEA) [5]. After implementing therapy for malignant neoplasms using antibodies in nuclear medicine, the notion arose of using this method for the development of tumour imaging based on target radionuclide delivery agents. Antibodies are used to transport drugs within organisms due to their specificity and affinity. Over the last three decades, considerable efforts have been made to develop visualization techniques using tracers based on antibodies labelled with different radionuclides [5,6]. Since their initial use, a relevant question has arisen concerning the strict compliance of the physical half-life of the radionuclide and the biology of the accumulation and half-lives of

[Downloaded from ijrr.com on 2026-11-03]
[DOR: 20.1001.1.23223243.2020.18.4.25.5]
[DOI: 10.52547/ijrr.18.4.825]

antibodies. In recent years, the most widely used radionuclides for imaging with antibodies are ^{111}In, ^{99m}Tc, ^{67}Ga, ^{86}Y, ^{64}Cu, and ^{124}I, with half-lives of 2.80 days, 6.0 h, 3.26 days, 14.74 h, 12.70 h, and 4.18 days, respectively [7].

However, each of these radionuclides has characteristics that limit their suitability for achieving visualization. For example, the radionuclide ^{64}Cu was successfully used as a radioactive label of antibodies in numerous preclinical studies in rodents. However, the half-life of ^{64}Cu 12.7 h is considered short given the slow pharmacokinetics for effective imaging visualization [8,9]. The radionuclide ^{86}Y has a half-life of 14.74 h, which is also too short to obtain high-quality images. The radionuclide ^{124}I has almost the perfect half-life (4.18 days) and has been effectively used for PET imaging with monoclonal antibodies [10,11]. However, due to the high energy of ^{124}I positrons (a maximum energy of E_{bmax}=2.1 Mev) and, consequently, their range in the tissue, the resolution of the resulting image is limited. The use of the radionuclide ^{99m}Tc has all the limitations specified for single-photon emission computed tomography. In addition, it has a half-life of 6.02 h, which is very short in terms of visualization when using antibodies [5].

Zirconium-89 (^{89}Zr) is a radiotracer possessing favourable attributes for antibody imaging. This radionuclide's half-life of 78.41 h is sufficient time to match the pharmacokinetics of antibody biodistribution. It exhibits good in-vivo stability with a low positron energy of 395 keV. Thus, the PET image resolution is satisfactory when using this radionuclide. In the intermediate state, ^{89m}Y is formed. In turn, ^{89m}Y decays ($T_{1/2}$=15.7 s) into the stable ^{89}Y by emitting gamma rays with energies of 909 Kev [7]. The physical half-life of zirconium-89 is well suited for PET visualization using antibodies [12]. These characteristics have stimulated increasing interest in ^{89}Zr: from a relatively little-known positron-emitting radioactive isotope less than ten years ago, it is currently the "ideal" isotope used in preclinical and clinical images in immuno-PET applications.

Zirconium-89 is used in PET visualization as a stable chelate bound to a monoclonal antibody [13]. When the zirconium is not bound to the chelate, it accumulates predominantly in bone tissue [14]. This is a particularly important factor in nuclear medicine. A high accumulation of ^{89}Zr in bone tissue with a clinical diagnosis restricts the range of applications for agents containing ^{89}Zr PET [13].

For labelling antibodies with radiometals, bifunctional chelates are often used, such as diethylenepentaacetic acid (DTPA) and desferal (DF). Three hydroxamate groups form the metal -binding moiety DF. Since it has been shown that zirconium (Zr) forms the most stable metal-hydroxamate complexes [13] and that Df has three hydroxamate groups, DF might be the chelate of choice for complexing Zr-89. The stability of the complex is compared with that of Zr-DTPA because DTPA-derivatives are commonly used bifunctional chelates for labelling antibodies with transition elements [13].

Monoclonal antibodies (MAbs) are a popular means of targeting cell surface antigens for therapeutic interventions and diagnostic imaging. MAbs have high affinity for their targets, and many have been developed as therapies for human patients. One disadvantage of their use includes their long serum clearance times, which necessitates protracted imaging spanning multiple days to clear background radioactivity [15, 16].

As mentioned in ICRP 128, "Radiolabelled monoclonal antibodies against antigenic substances within or on the surface of malignant cells are used in medical research and for diagnosis and treatment of cancer. The antibody is an immunoglobulin, usually IgG_1 or IgG_{2a} and is used either as the intact molecule (molecular weight 150 kDa) or as fragments $F(ab')_2$ (100 kDa) and F(ab') (50 kDa) [17, 18]. Intact MAb remains in the human body from several days to several weeks, which leads to optimal accumulation in tumour relative to non-tumour site during 2-4 days after injection" [18].

To utilize any radiopharmaceuticals, assessment of the absorbed dose in organs and tissues is required. In the literature, there is very little data on dose assessment for the use of MAbs and their fragments labelled with ^{89}Zr. ICRP publication 128 [18] presents data on the

[Downloaded from ijrr.com on 2026-11-03]

[DOR: 20.1001.1.23223243.2020.18.4.25.5]

[DOI: 10.52547/ijrr.18.4.825]

dynamic behaviour of antibodies labelled with the radionuclides ^{99m}Tc, ^{131}I, ^{111}In, and ^{123}I, providing a reference character for MAbs and their labels. In this report, data for ^{89}Zr are absent. It should be noted that the biological rates of radionuclide removal from an organ are determined not by the nuclide properties but by the properties of the carrier (MAb) to which they are attached. As such, all coefficients of the use of ^{89}Zr are considered to be that given in ICRP 128 for ^{99m}Tc, as well as for all listed radionuclides [18-19].

Currently, dosimetry for ^{89}Zr-labelled monoclonal antibodies has been insufficiently studied. For effective PET imaging, assessment of the absorbed dose on the most highly exposed organs and tissues, as well as the effective dose assessment, is required.

In this work, ICRP information on the MAb biokinetic model was used to present a biokinetic model for ^{89}Zr-labelled intact monoclonal antibodies. This biokinetic model was subsequently modified with published real experimental results on the dosimetry of ^{89}Zr-labelled monoclonal antibodies in order to improve it. The results from the developed model are compared with other real and simulated models.

MATERIALS AND METHODS

Theoretical assumptions from the biokinetic model

The objective of this study is a general assessment of the radiation exposure of organs and tissues without connection to specific monoclonal antibodies. The original averaged data for the calculations of the half-life values of the radiotracer from the bloodstream in connection with the transition to tissues and organs was taken at 50 h for an intact MAb [24-27]. The biological removal times of 24 and 96 h in F_s (the fractional distribution to organ or tissue) were taken from ICRP 128 [18].

With respect to antibody behaviour, there are some common features. After intravenous injection, the highest activity is observed in organs with high vascular perfusion, such as the liver, spleen, bone marrow, and kidneys [17, 18]. For intact antibodies, there are two elimination rates: from blood to organ and from blood to tissues. Based on this approach, a model of radionuclide behaviour in the body was developed. The biokinetic model of the behaviour of ^{89}Zr associated with intact antibodies is shown in figure 1.

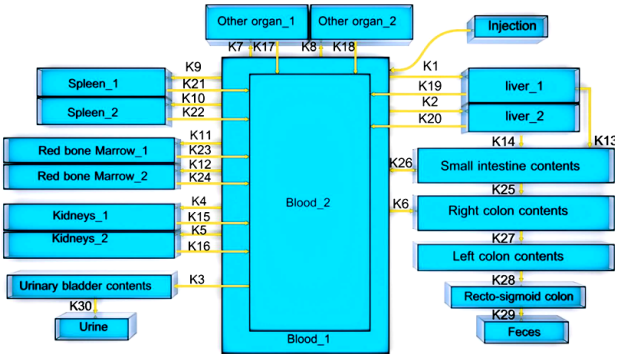


Figure 1. The biokinetic model based on ICRP128 information for 89Zr associated with intact antibodies with two elimination rates: from blood to organ and from blood to tissue.

In this biokinetic model, the compartment from which there is a transition is designated as "Blood_1." It was initially introduced in the form of compound-labelled intact MAb. Upon receipt of the compound into the organ, reverse excretion is associated with the metabolism of antibodies and the release of the radio nuclide. However, it is recommended in an earlier publication [18] that, after releasing antibodies or their fragments from ^{99m}Tc, a biokinetic model for pertechnetate should be used: when ^{111}In is released, the biokinetic model for indium in ionic form should be used. The most commonly used form of ^{89}Zr for labelling MAb is its binding to chelating compounds, for which desferrioxamine (DFO) has been commonly used [13]. Zr-DFO exhibits good stability with respect to demetallization, releasing less than 0.2% of the metal in blood plasma after 24 hours [13]. Since zirconium remains bound to the chelate, a scheme of characteristics of ionic zirconium was not used to describe its excretion [23]. Rather, a scheme of characteristics for the behaviour of chelate complexes was implemented. Traditionally, chelate complexes are used to excrete plutonium from the body: this excretion

[Downloaded from ijrr.com on 2026-11-03]
[DOR: 20.1001.1.23223243.2020.18.4.25.5]
[DOI: 10.52547/ijrr.18.4.825]

has been better studied. Therefore, excretion from the organs and tissues does not go to the "blood-1" compartment, but to the "blood-2" compartment. Note that the "blood-1" and "blood-2" compartments are not two different blood systems, but rather illustrate that the compound has different behaviour patterns during insertion and excretion. The constant for the excretion of the chelate complex is taken from an earlier study [29]. The rates of passage through the gastrointestinal tract and urinary excretory system are standard and are given in earlier publications (ICRP Publication 30, 1972; ICRP Publication 67, 1993; ICRP Publication 100) [20].

Absorbed dose calculation

To calculate the absorbed dose in organs and tissues, there are two possible approaches. In the first, based on the transfer activity fraction from blood to organs and removal activity rate from organs and the excretion rate, the WinAct program [32] (https://www.ornl.gov/crpk/software) is used to calculate the cumulative activity in organs and tissues [33]. The output results from the WinAct program are used as input data for IDAC 2.1 software, an internal dosimetry program for nuclear medicine based on the ICRP adult reference voxel phantoms [34], [35]. As a result, the absorbed doses to organs and tissues are estimated.

In the second approach, the cumulative activity is directly calculated with equation (1) [18]. The absorbed dose to organs and tissue is estimated directly with IDAC 2.1 by using equation 1:

$$\frac{\tilde{A}_s}{A_0} = F_S \sum_{i=1}^{n} a_i \frac{T_{i,eff}}{\ln(2)} \qquad (1)$$

Where F_s is the fraction of the administered substance that would arrive in source organ or tissue S over time if there were no radioactive decay, a_i is the fraction of F_s eliminated with a biological half-time T_i ($\Sigma a_{i=1}$), n is the number of elimination components, and $T_{i,eff}$ is the uptake effective half-times. This equation is used by ICRP128 [18].

The effective half-time can be calculated from the corresponding biological half-time T_i and the functional physical half-life T_p with the use of equation 2:

$$T_{eff} = \frac{T_i \cdot T_p}{T_i + T_p} \qquad (2)$$

In cases when the retention function cannot be described by a sum of exponential functions, the cumulated activities are directly derived from the metabolic model. For absorbed dose calculations in nuclear medicine, it has often been assumed that the effective half-time in an organ equals the physical half-life. The reason for this approximation is that the substance, in these cases, is labelled with a radionuclide with a physical half-life that is short in comparison with the biological half-time. For short-lived radionuclides, a slow biological excretion may not be apparent; for absorbed dose calculations, the approximation is sufficiently accurate [18].

Modified biokinetic model with real results

Lindenberg *et al.* (2017) [16] calculate the maximum dosing for effective imaging with minimal radiation exposure in a small subset. In this work, three patients with metastatic colon cancer were injected with approximately 1 mCi (37 MBq) of ^{89}Zr-panitumumab IV. Whole body static images were then obtained at 2-6 hours, 1-3 days, and 5-7 days post injection. Whole organ contours were applied to the liver, kidneys, spleen, stomach, lungs, bone, gut, heart, bladder, and psoas muscle. From these contours, time activity curves were derived and used to calculate mean resident times. These authors used the mean resident times as input for OLINDA 1.1 software in order to provide dosimetry estimates. The organ with the highest dose was the liver. The effective dose is within the range of estimates extrapolated from mice studies. This study concludes that ^{89}Zr-panitumumab appears safe and the dosimetry estimates are reasonable for clinical imaging. Based on the results from real human diagnosis and administration in Lindenberg *et al.* (2017) [16], the utilized biokinetic model in figure 1 was modified to the model in figure 2. New organs

[Downloaded from ijrr.com on 2026-11-03]
[DOR: 20.1001.1.23223243.2020.18.4.25.5]
[DOI: 10.52547/ijrr.18.4.825]

(lungs, heart wall, bone, and stomach) are added depending on the impact of these organs in the actual experimental data from three patients under investigation. Activity in these organs was measured, and the absorbed fraction from the experimental results was used. In reference [16], the measured activity of three real patients for each organ was contoured on PET images three times (12, 30, and 150 h). Hence, the biological removal half-life ($T_{1/2}$) of intact MAb from the bloodstream is assumed to be 50h (as in the first model). Two biological removal half-times, 18 and 138 h (based on previously published experimental results), [16] were assessed.

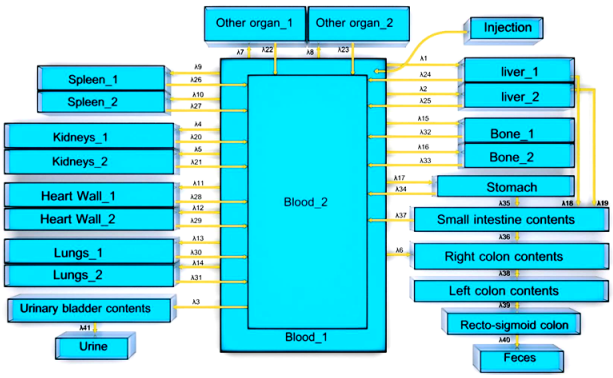


Figure 2. The modified biokinetic model of the behaviour of 89Zr associated with intact antibodies based on real clinical results from Lindenberg et al. (2017) (16).

RESULTS AND DISCUSSION

Figures 3 and 4 refer to the time-activity curves of the intact radiopharmaceutical as fitted by WinAct. The figures show the intact MAb labelled with ^{89}Zr accumulate in organs relative to the excretion of the radionuclide from those same organs.

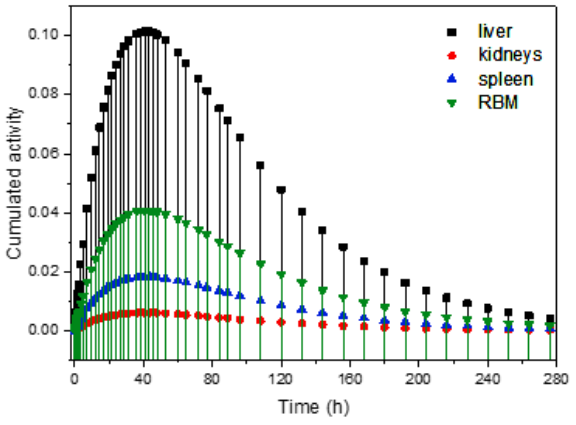


Figure 3. Fractional activity as a function of time (h) for the liver, kidneys, spleen, and red bone marrow from WinAct.

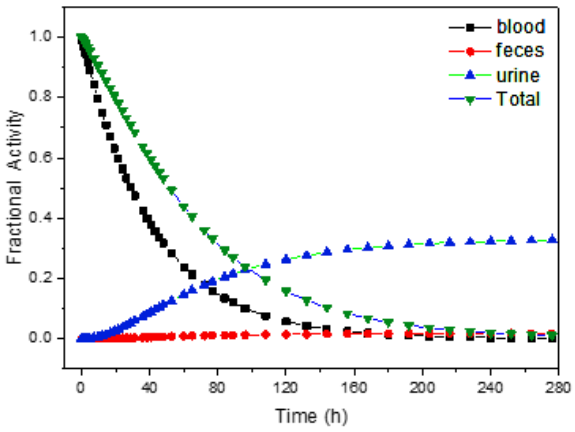


Figure 4. Fractional activity as a function of time (h) for blood, excretions, and total organs from WinAct.

To assess the level of risk from radiation exposure to the patient due to radiopharmaceutical use, absorbed doses were calculated for organs where the labelled complex accumulates to the greatest extent, namely, the kidneys, red bone marrow, spleen, and liver. Since the ^{89}Zr isotope decays by emitting gamma rays, and gamma rays result from positron annihilation, it was also necessary to calculate absorbed doses in adjacent organs (targeted organ) which received radiation from source organs. Connected with this, doses in the lungs from the radionuclide in the liver, as well as doses in the gonads from the contents of the bladder, were calculated as the most closely related organs. The injection was administered directly into the blood, which circulates throughout the body and, to a large extent, the lungs. Therefore, we also assessed the absorbed dose. Additionally, the contribution to the lungs, red bone marrow, and gonads from "other organs and tissues" was assessed. The results showed that for the rest of the internal organs, the contribution to the dose was less than for the listed organs by one or two orders of magnitude, so a detailed calculation of the doses was not performed.

Calculations were made for an injection of an intact antibody labelled with ^{89}Zr. The

[Downloaded from ijrr.com on 2026-11-03]
[DOR: 20.1001.1.23223243.2020.18.4.25.5]
[DOI: 10.52547/ijrr.18.4.825]

cumulative activity data and numerical values of the dose coefficients for the intact antibody labelled with ^{89}Zr are presented in table 1.

Table 1. Cumulative activity in organs of the intact antibody labelled with ^{89}Zr (normalized to 1 Bq of injected activity) and the numerical values of the dose coefficients of N radionuclide ^{89}Zr in organs and tissues.

ORGANS OR TISSUES	Cumulative Activity (Bq/day)	Dose Coefficient (mGy/MBq)
Blood	1.50E+05	-
Liver	4.42E+04	1.33E+00
Red bone marrow	1.78E+04	8.24E-01
Other organs and tissues	1.60E+04	-
Spleen	8.00E+03	1.54E+00
Kidneys	2.67E+03	8.01E-01
Urinary bladder contents	2.39E+03	2.85E-01
Small intestine contents	6.25E+00	4.36E-01
Left Colon_cont	1.42E+03	4.85E-01
Right Colon_cont	9.70E+02	5.33E-01
Lung	-	6.60E-01
Heart wall	-	9.79E-01
Stomach wall	-	6.75E-01
Testes	-	1.16E-01
Thymus	-	1.92E-01
Thyroid	-	2.93E-01
Tongue	-	1.77E-01

The injection activity for imaging tumours using the ^{89}Zr isotope varied from 37 to 75 MBq [27]. In this case, when using radiopharmaceuticals in the form of intact antibodies with an activity of 75 MBq, the absorbed dose in the spleen was 115 mGy and 100 mGy in the liver.

Figure 5 presents the dependence of absorbed doses in the organs at different removal half-lives $T_{1/2}$ of activity from blood to organ and tissues. As shown, for the liver there was no significant dependence of the absorbed doses on removal half-time (the difference between $T_{1/2}$=12 to $T_{1/2}$=150 was no more than 10%)[37]. For the other organs, the difference reached 30-40%: in some organs, such as red bone marrow, alveolar-interstitial, heart wall, and lungs, the value was doubled. In this case, the presented model could be used for other types of monoclonal antibodies, not only for panitumumab MAb.

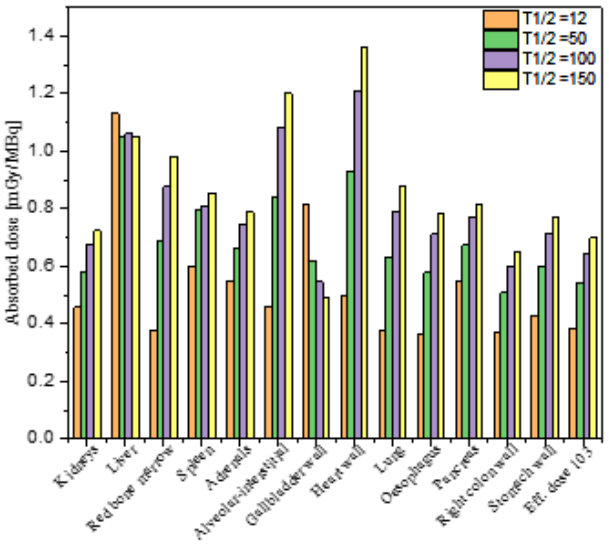


Figure 5. Absorbed dose in mGy/MBq of Zr-89 MAb for adult males at different clearance times from blood.

Figure 6 shows the results of comparing the dose calculation conducted using the two approaches discussed above:

- The use of a biokinetic model and solving a system of differential equations with the use of WinAct;
- Direct calculation of residence time based on thr initial parameters from the ICRP 128 report.

In both cases, the IDAC 2.1 software was used for dose calculations in organs and tissues. The results revealed close values of absorbed doses for all organs, except the liver, spleen, and gallbladder [38]. This illustrates that the most exposed organs are the spleen, liver, kidneys, red marrow, and lungs for an administered ^{89}Zr injection in the body bound to intact MAb. The WinAct program method of calculating the cumulative activity is more accurate, as the fraction distribution, F_s, is described and calculated for organs not only for intake (as in the ICRP model) but also for elimination.

Modified Biokinetic model

With the modified biokinetic model, the half-life values of the radiotracer from the bloodstream in connection with the transition to the organs and tissues were taken at 12 h for the

[Downloaded from ijrr.com on 2026-11-03]

[DOR: 20.1001.1.23223243.2020.18.4.25.5]

[DOI: 10.52547/ijrr.18.4.825]

intact MAb [16]. The biokinetic data, such as the biological removal half-times, were 18 and 138 h [16]. F_s represents the fractional distribution to organ or tissue [18]. The obtained absorbed dose with the developed biokinetic model for different organs and tissues is listed in table 3. The highest doses were for the liver, gallbladder wall, spleen, pancreas, and kidneys (1.07, 0.77, 0.70, 54, and 0.44 mGy/MBq, respectively).

In the study by Lindenberg *et al.* (2017), the cumulative activity was shown as a formula of resident time and was presented for human diagnostics. In addition, in this paper these data were used to calculate organ absorbed dose with the program OLINDA 1.1 [16]. The OLINDA personal computer code was created as a replacement for the widely used MIRDOSE3.1 code. This is useful for standardizing and automating internal dose calculations, assessing doses in clinical trials with radiopharmaceuticals, making theoretic calculations for existing pharmaceuticals, teaching, and other purposes [36].

In the present work, the absorbed dose was calculated with IDAC 2.1 directly from the resident time mentioned in the previous study [16], and the results were compared with those obtained from the modified model using WinAct 1.1 and equation (1) in the IDAC 2.1 program. The results were s compared, as shown in figure 7, with the OLINDA 1.1 results mentioned in paper [16].

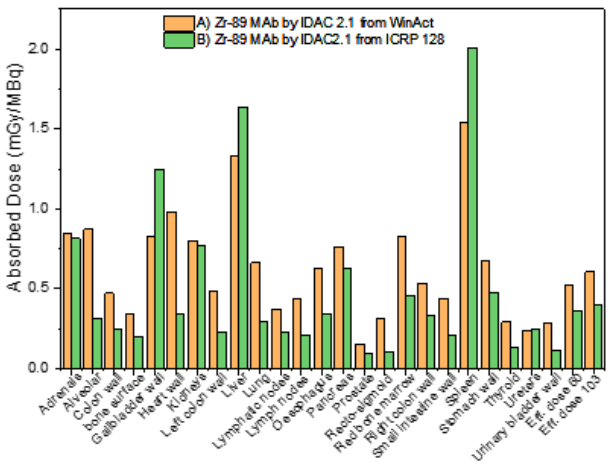


Figure 6. Bar chart plots of the estimated absorbed doses to the mean organs for adult males using two calculation methods; a) cumulative activity calculated by the WinAct program and insertion of IDAC 2.1; b) cumulative activity calculated directly with equation (1) from ICRP128 and then inserted into IDAC 2.1.

Table 3. Cumulative activity in organs of the intact antibody labelled with 89Zr (normalized to 1 Bq of injected activity) and numerical values of dose coefficients of N radionuclide 89Zr in organs and tissues with the developed biokinetic model.

ORGANS OR TISSUES	Cumulative Activity	Dose Coefficient (mGy/MBq)
Blood	1.50E+05	_
Bone	4.80E+02	_
Adrenals	_	6.64E-01
Other organs and tissues	5.77E+04	_
Brain	_	1.43E-01
Breast	_	2.28E-01
Bronchi Bound	_	5.18E-01
Bronchi Sequestered	_	5.18E-01
Colon Wall	_	4.58E-01
Endosteum (Bone Surface)	_	3.12E-01
Eye Lenses	_	7.77E-02
Gallbladder Wall	_	6.21E-01
Heart Wall	1.85E+02	9.31E-01
Kidneys	5.55E+02	5.80E-01
Left Colon_Cont	1.59E+03	
Left Colon Wall	_	4.72E-01
Liver	3.01E+04	1.05E+00
Lung	5.33E+02	6.31E-01
Lymphatic Nodes	_	3.56E-01
Muscle	_	1.73E-01
Oesophagus	_	5.76E-01
Pancreas	_	6.74E-01
Pituitary Gland	_	1.16E-01
Prostate	_	1.81E-01
Recto-Sigmoid Colon Wall	_	3.31E-01
Red (Active) Bone Marrow	_	6.85E-01
Right Colon_Cont	1.09E+03	_
Right Colon Wall	_	5.08E-01
Salivary Glands	_	1.07E-01
Skin	_	1.46E-01
Small Intestine_Cont.	4.66E+01	_
Small Intestine Wall		4.27E-01
Spleen	2.24E+03	7.94E-01
Stomach Wall	1.16E+01	5.98E-01
Testes	_	1.58E-01
Thyroid	_	3.00E-01
Ureters	_	2.22E-01
Urinary Bladder_Cont.	2.31E+03	_
Urinary Bladder Wall	_	3.01E-01
Effective Dose 60 [mGy/MBq]	_	4.53E-01
Effective Dose 103 [mGy/MBq]	_	5.42E-01

[Downloaded from ijrr.com on 2026-11-03]
[DOR: 20.1001.1.23223243.2020.18.4.25.5]
[DOI: 10.52547/ijrr.18.4.825]

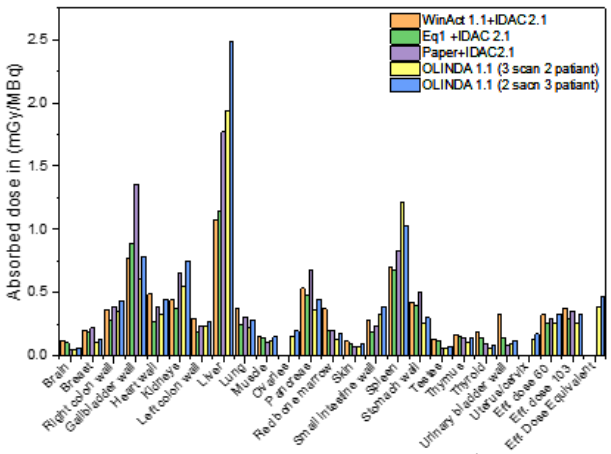


Figure 7. Comparison of absorbed dose in mGy/MBq of Zr-89 MAb for adult males using four calculation techniques.

The effective dose was compared, and there was good agreement between the results from the developed model and the results measured directly from Lindenberg *et al.* (2017) [16] using OLINDA 1.1. In the liver, based on the residence time given in the study, the results were nearly the same in OLINDA 1.1 and IDAC 2.1. The differences between the study's data and our modelling calculation were also clear for the liver. For the kidneys, the difference was not significant and can be considered negligible. Only in the spleen did the OLINDA 1.1 program give excess doses. It is difficult to estimate the reason for this discrepancy because the modelling approach and data on residence time from the study are in good agreement.

In general, the modified biokinetic model is in good agreement with direct measurements performed in patients and can be considered as a first step in the dosimetry simulation of ^{89}Zr-labelled monoclonal antibodies.

CONCLUSION

The dynamics of the behaviour in the body of a radiopharmaceutical based on ^{89}Zr-labelled antibodies were considered, and a biokinetic model constructed. For the ^{89}Zr-labelled monoclonal antibodies, the most exposed organs are the spleen, liver, kidneys, red marrow, and lungs. The created model was developed according to newly published results from real patients injected with ^{89}Zr-labelled monoclonal antibodies. The developed biokinetic model is in good agreement with the direct measurements and can be considered as a first step in the radiopharmaceutical dosimetry simulation of the ^{89}Zr isotope.

***Conflicts of interest*:** *Declared none.*

REFERENCES

1. Demlova R, Valík D, Obermannova R, Zdražilová-Dubská L (2016) The safety of therapeutic monoclonal antibodies: Implications for Cancer Therapy Including Immuno-Checkpoint Inhibitors Monoclonal antibodies in cancer. *Physiol Res,* **65**: 455–462.
2. Catapano AL and Papadopoulos N (2013) The safety of therapeutic monoclonal antibodies: Implications for cardiovascular disease and targeting the PCSK9 pathway. *Atherosclerosis, **228(1)**: 18–28*.
3. Geskin LJ (2015) Monoclonal Antibodies. *Dermatol Clin, **33 (4)**: 777–786*.
4. Liu JKH (2014) The history of monoclonal antibody development - Progress, remaining challenges and future innovations. *Ann Med Surg, **3(4)**: 113–116*.
5. Wu AM and Senter PD (2005) Arming antibodies: Prospects and challenges for immunoconjugates. *Nature Biotechnology, **23**: 1137–1146*.
6. Wu AM (2014) Engineered antibodies for molecular imaging of cancer. *Methods*, ***65(1)**: 139-147*.
7. Wadas TJ Wong EH Weisman GR Anderson CJ (2010) Coordinating radiometals of copper, gallium, indium, yttrium, and zirconium for PET and SPECT imaging of disease. *Chem Rev, **110(5)**:2858–2902*.
8. Cai W, Chen K, He L, Cao Q, Koong A, Chen X (2007) Quantitative PET of EGFR expression in xenograft-bearing mice using64Cu-labeled cetuximab, a chimeric anti-EGFR monoclonal antibody. *Eur J Nucl Med Mol Imaging, 3**4(6)**: 850–858*.
9. Paudyal P, Paudyal B, Oriuchi N, Iida Y (2010) Imaging and biodistribution of Her2 / neu expression in non-small cell lung cancer with 64 Cu labeled trastuzumab PET. *Cancer Sci, **101(4)**: 1045-50*.
10. Börjesson PKE, Jauw YWS, Boellaard R, *et al.* (2006) Performance of immuno-positron emission tomography with zirconium-89-labeled chimeric monoclonal antibody U36 in the detection of lymph node metastases in head and neck cancer patients. *Clin Cancer Res, **12(7 Pt 1)**: 2133–40*.
11. Verel I, Visser GWM, Vosjan MJWD, Finn R, Boellaard R, *et al.* (2004) High-quality124I-labelled monoclonal antibodies for use as PET scouting agents prior to131I-radioimmunotherapy. *Eur J Nucl Med Mol Imaging, **31**:*

[Downloaded from ijrr.com on 2026-11-03]
[DOR: 20.1001.1.23223243.2020.18.4.25.5]
[DOI: 10.52547/ijrr.18.4.825]

1645–1652.
12. Holland JP, Williamson MJ, Lewis JS (2010) Unconventional Nuclides for Radiopharmaceuticals. *Mol Imaging*, ***9(1)****: 1–20*.
13. Meijs WE, Herscheid JDM, Haisma HJ, Pinedo HM (1992) Evaluation of desferal as a bifunctional chelating agent for labeling antibodies with Zr-89. *Int J Radiat Appl Instrumentation Part,* ***43(12)****: 1443–1447*.
14. Fletcher CR (1969) The radiological hazards of zirconium-95 and niobium-95. *Health Phys,* ***16(2)****: 209–220*.
15. Chiavenna SM, Jaworski JP, Vendrell A (2017) State of the art in anti-cancer mAbs. *J Biomed Sci,* ***24(1)***.
16. Lindenberg L, Adler S, Turkbey IB, Mertan F, *et al.* (2017) Dosimetry and first human experience with 89Zr-panitumumab. *Am J Nucl Med Mol Imaging,* ***7(4)****: 195–203*.
17. Fischman AJ, Khaw BA, Strauss HW (1989) Quo vadis radioimmune imaging. *J Nucl Med,* ***30(11)****: 1911–5*.
18. ICRP Publication 128 (2015) Radiation Dose to Patients from Radiopharmaceuticals: A Compendium of Current Information Related to Frequently Used Substances. *Ann ICRP,* ***44(2_suppl)****: 7–321*.
19. Mostafa MYA, Zakaly HMH, Zhukovsky M (2019) Assessment of exposure after injection of 99mTc-labeled intact monoclonal antibodies and their fragments into humans. *Radiol Phys Technol,* ***12(1)****: 96–104*.
20. Vennart J (1981) Limits for intakes of radionuclides by workers: ICRP publication 30. *Health Phys,* ***40(4)****: 477–484*.
21. Leggett RW (2008) The biokinetics of inorganic cobalt in the human body. *Sci Total Environ,* ***389(2–3)****: 259–269*.
22. Leggett RW (2012) A biokinetic model for zinc for use in radiation protection. *Sci Total Environ*, ***420****: 1-12*.
23. Li WB, Greiter M, Oeh U, Hoeschen C (2011) Reliability of a new biokinetic model of zirconium in internal dosimetry: Part II, parameter sensitivity analysis. *Health Phys,* ***101(6)****: 677–692*.
24. Carrasquillo JA, Pandit-Taskar N, O'Donoghue JA, Humm JL, *et al.* (2011) 124I-huA33 Antibody PET of Colorectal Cancer. *J Nucl Med*, ***52(8)****: 1173-80*.
25. Klibanov AL, Martynov AV, Slinkin MA, IYu S, *et al.* (1988) Blood clearance of radiolabeled antibody: enhancement by lactosamination and treatment with biotin-avidin or anti-mouse IgG antibodies. *J Nucl Med,* ***29(12)****: 1951–1956*.
26. Mould DR and Sweeney KRD (2007) The pharmacokinetics and pharmacodynamics of monoclonal antibodies - Mechanistic modeling applied to drug development. *Curr Opin Drug Discov Dev,* ***10(1)****: 84–96*.
27. Dijkers EC, Oude Munnink TH, Kosterink JG, Brouwers AH, *et al.* (2010) Biodistribution of 89Zr-trastuzumab and PET imaging of HER2-positive lesions in patients with metastatic breast cancer. *Clin Pharmacol Ther,* ***87(5)****: 586–592*.
28. Buchmann I, Kull T, Glatting G, Bunjes D, *et al.* (2003) A comparison of the biodistribution and biokinetics of99mTc -anti-CD66 mAb BW 250/183 and99mTc-anti-CD45 mAb YTH 24.5 with regard to suitability for myeloablative radioimmunotherapy. *Eur J Nucl Med Mol Imaging*, **30(5)***: 667-73*.
29. Khokhryakov VF, Belyaev AP, Kidryavtseva TI, Schadilov AE, *et al.* (2003) Successful DTPA therapy in the case of 239Pu penetration via injured skin exposed to nitric acid. *Radiat Prot Dosimetry,* ***105(1–4)****: 499–502*.
30. ICRP Publication 30 (1972) Limits for Intakes of Radionuclides by Workers. *Ann ICRP*:Ann. ICRP, ***2****: (3-4)*.
31. ICRP Publication 67 (1993) Age-dependent Doses to Members of the Public from Intake of Radionuclides - Part 2 Ingestion Dose Coefficients. *Ann ICRP*: Ann. *ICRP,* ***23****: (3-4)*.
32. Oak Ridge National Laboratory (2002) No Title.
33. Eckerman KF and Leggett RW (2002) WinAct.
34. Andersson M, Johansson L, Eckerman K, Mattsson S (2017) IDAC-Dose 2.1, an internal dosimetry program for diagnostic nuclear medicine based on the ICRP adult reference voxel phantoms. *EJNMMI Res,* ***7(1)****: 88*.
35. ICRP (2009) Adult Reference Computational Phantoms ICRP. *Ann ICRP, 110(39 (2)): 162*.
36. Stabin MG, Sparks RB, Crowe E (2005) OLINDA/EXM: The Second-Generation Personal Computer Software for Internal Dose Assessment in Nuclear Medicine. *J Nucl Med*, ***46 (6)****: 1023–1028*.
37. Zakaly H, Mostafa M, Deryabina D, Zhukovsky M (2020) Comparative Studies on the Potential Use of 177Lu-Based Radiopharmaceuticals for the Palliative Therapy of Bone Metastases. *Int J Radiat Biol, https://doi.org/10.1080/09553002.2020.1729441*
38. Zakaly HMH, Mostafa MYA, Zhukovsky M (2019) Dosimetry Assessment of Injected 89Zr-Labeled Monoclonal Antibodies in Humans. *Radiat Res,* ***191:*** *466–474*

[Downloaded from ijrr.com on 2026-11-03]
[DOR: 20.1001.1.23223243.2020.18.4.25.5]
[DOI: 10.52547/ijrr.18.4.825]

[DOI: 10.52547/ijrr.18.4.825] [DOR: 20.1001.1.23223243.2020.18.4.25.5] [Downloaded from ijrr.com on 2026-11-03]